Journal of the European Ceramic Society 16 (1996) 857–864

0955-2219(95)0206-5
0955-2219/96/$15.00 +.00

# A Statistical Analysis of the Influence of Processing Conditions on the Properties of Fused Silica

D Kićević, M. Gašić & D. Marković

The Institute of Nuclear Sciences 'Vinča', Materials Science Laboratory, P.O.B. 522, 11001 Belgrade, Serbia

(Received 29 September 1995; accepted 4 November 1995)

***Abstract***

*In this work the quantitative relations between the properties of sintered fused silica (density, mechanical properties, cristobalite content) and slip preparation parameters as well as sintering conditions (milling balls material, temperature and time of sintering) were established. Multifactorial experimental design was used in order to obtain the respective mathematical models. The response surfaces of these models were analyzed, together with correlations between the compressive and tensile strength and cristobalite content. It was established that the maximum values of mechanical properties for a given material were obtained with 6–8 vol.% of cristobalite in sintered samples.*

*Les relations quantitatives entre les caractéristiques des échantillons frittés (la densité, les caractéristiques mécaniques, le contenu de cristobalite) et les paramétres de la préparation de la suspension de coulage et les conditions de frittage (le materiel des balles de moulage, la température et le temps de frittage) ont étés établies. Pour obtenir des modèles mathématiques, un dessin expérimentale multifactoriel a été utilisé. Les surfaces de reponse de ces modèles ont été analysées avec la corrélation entre les résistances sous pression et sous tension et le contenu de cristobalite. On a été trouvé que le maximum des caractéristiques mécaniques peut être gagné avec un contenu de cristobalite de 6–8% vol. dans des échantillons frittés.*

*In dieser Arbeit werden quantitative Zusammenhänge zwischen den Eigenschaften von gesintertem Siliziumdioxid (Dichte, mechanische Eigenschaften, Cristobalitgehalt) und den Bedingungen für die Vorbereitung des Schlickers und für das Sintern (Mahlkugelnmaterial, Sintertemperatur und - zeit) festgestellt. Es werden Vielfaktorenversuchspläne benutzt, um entsprechende statistische Modelle zu erstellen. Echooberflächen dieser Modelle werden zusammen mit Abhängigkeiten zwischen Druckfestigkeit und Zugfestigkeit einerseits und Cristobalitgehalt andererseits analysiert. Es wurde festgestellt, daß die maximalen Werte der mechanischen Eigenschaften für ein Material mit 6–8 vol.% Cristobalit in den gesinterten Proben erreicht wird.*

## 1 Introduction

Fused silica ceramics have found quite broad application due to the good combination of its properties (refractoriness, thermal shock resistance, and good mechanical properties at elevated temperatures).[1–4] The forming of fused silica products is done mostly by slip-casting. The preparation of the slip comprises: (a) wet-milling of coarse fused silica powder to obtain required particle size distribution; (b) slip stabilization for adjusting slip viscosity. After drying the green casts are subjected to sintering, in order to improve mechanical properties.

The fused silica sintering mechanism is viscous flow as for all glassy materials, if there is no significant devitrification to cristobalite. This process depends on many factors: chemical purity, temperature, time, heating conditions, atmosphere, particle size, porosity of green casts etc.[1–5] During sintering of fused silica two processes occur: (a) increase of strength as a result of the strengthening of the contacts between particles and porosity decrease; (b) decrease of strength, as a result of pronounced devitrification, and consequent flaw initiation because of cristobalite phase transformation upon cooling.[5] In this way all parameters that can affect devitrification can affect also sintering.

Indirectly, these two processes are influenced by slip preparation parameters (material of milling balls, mill loading coefficient, rotation speed, solid phase content in the slip, grain size distribution of starting material, pH etc.), through resulting content of impurities ($Na_2O$, $K_2O$, $CaO$, $Al_2O_3$ etc).[6,7] and grain size distribution of the slip. Using high purity materials, the devitrification problem can be avoided, but in broader applications (metallurgy,

chemical and glass industry and similar) the 'technical grade' fused silica materials of different purity are more frequently used. Therefore, it is necessary for every single material to establish the proper conditions for sintering (temperature, time etc.).[2–5]

In this work, investigation of the influence of most significant process parameters of fused silica sintering (impurity content in casting slip as a result of different milling ball material, sintering temperature and soaking time) on the properties of sintered fused silica (density, open porosity, strength and cristobalite content) was performed. Statistical models, giving quantitative relations between investigated process parameters (influencing factors) and related properties (system responses), were established on the basis of multifactorial experimental design. These quantitative relations enabled the determination of the optimum sintering conditions for investigated material.

## 2 Experimental Work

The coarse fused silica powder of technical grade purity was used (Elmin, The Netherlands). The properties of this powder are given in Tables 1 and 2.

Slips were prepared by wet-milling of coarse powder in a porcelain mill with silica balls (99% $SiO_2$) and alumina balls (70% $Al_2O_3$). Solid content in the slip was 82% mass and deflocculant Dispex 115N (Progress Engineers Ltd, Stoke-on-Trent, UK) was added (1% of solid content). Balls to slip ratio was between 1·25 and 1·5 and rotation speed was 4·2 rad/s (40 rpm). The milling time was 25% shorter for $Al_2O_3$ balls, for slips having the similar grain size distribution after milling (90–95% smaller than 63 μm, 80–90% smaller than 30 μm).

After milling, the slips were stabilized by rotating for up to 30 h in the mill without balls, when they were ready for casting, having density of 1·83 g/cm$^3$ and viscosity of about 300 mPas (Brookfield viscometer RVT (spindle 4), Stoughton, Mass. USA).

Slip casting was performed into the impregnated plaster moulds. The obtained casts ($\phi$ 20 × 100 mm) were dried in air for 24 h, then for 24 h at 110°C and finally 4 h at 180°C. The density of the dry casts was 1·89 g cm$^{-3}$.

**Table 1.** Chemical composition of fused silica powder

| Component | $SiO_2$ | $Al_2O_3$ | $Fe_2O_3$ | CaO | $Na_2O$ | $K_2O$ |
|---|---|---|---|---|---|---|
| Content (%) | 99·02 | 0·43 | 0·04 | 0·43 | 0·05 | 0·02 |

**Table 2.** Particle size distribution of fused silica powder

| Particle size (mm) | <0·3 | 0·3–0·6 | 0·6–1 | 1–2 | 2–3 | >3 |
|---|---|---|---|---|---|---|
| Content (%) | 1 | 7 | 22 | 37 | 32 | 1 |

The firing of samples was performed in a tubular furnace, in air, with heating rate of 200°C/h. The soaking times at temperatures 1175 and 1275°C were 1 and 3 h. After that samples were quenched down to room temperature in air. Such a cooling procedure was recomended for establishing the optimum sintering conditions.[2]

Density and open porosity of sintered samples were measured by immersion in xylene. Compressive strength was determined by standard measurement on cylindrical samples (diameter 20 mm, height 10 mm). It was calculated from the relationship between crushing force and sample cross area ($D^2\pi/4$). Tensile strength was determined by the diametral compression method[8] on the same samples, but with diametral loading (perpendicular to compressive strength loading). Using special hard paper attachments shear stress concentration was avoided. Tensile strength was calculated from the following relationship:

$$\sigma_{tens} = \frac{2F}{\pi D H} \quad (1)$$

where: $\sigma_{tens}$ — tensile strength;
$F$ — crushing force;
$D$ — sample diameter;
$H$ — sample height.

Cristobalite content was determined by the modified Harris and Welsh method.[9] This is a quantitative X-ray diffraction method, measuring the integral number of impulses in the interval $2\Theta$ from 21 to 23° (characteristic reflection of the plane (101) for β-cristobalite at $2\Theta$ = 21·94°) on sintered samples and specially prepared standards.[10]

The chemical analysis of green casts, made by atomic absorption spectroscopy, is shown in Table 3. It is evident that higher impurity content is produced with $Al_2O_3$ balls.

## 3 Results, Discussion and Statistical Modelling

The properties of samples sintered under different processing conditions are presented in Table 4. A combination of processing parameters was set up following the special design of the experiments, enabling us to investigate the influence of these parameters on sintered fused silica properties through the established statistical models.

### 3.1 Statistical models and their analysis

The statistical method of multifactorial experimental design[8,9] was used in order to obtain the empirical models for relations between properties of sintered samples (system responses) and some process parameters (influencing factors) in an efficient way, i.e. with as little experimentation as possible. Box–Wilson

**Table 3.** Chemical composition of the green casts as a function of ball milling material

| *Ball Milling material* | *Composition (%)* | | | | | | |
|---|---|---|---|---|---|---|---|
| | $SiO_2$ (from difference) | Impurities (total) | $Al_2O_3$ | $Fe_2O_3$ | CaO | $Na_2O$ | $K_2O$ |
| $SiO_2$ | 99·17 | 0·83 | 0·25 | 0·04 | 0·49 | 0·04 | 0·01 |
| $Al_2O_3$ | 98·75 | 1·25 | 0·53 | 0·05 | 0·59 | 0·06 | 0·02 |

orthogonal plans[11,12] were used with some adopted modifications because of the specific nature of one influencing factor — ball milling material. A slightly modified matrix plan $2^3$ — three factors on two levels was used (the coding of factors and system responses is given in Table 5). Established empirical statistical models have the general form:

$$Y = b_0 + \Sigma b_i x_i + \Sigma b_{ij} x_i x_j + \ldots\ldots\ldots \quad (2)$$

in which regression coefficients ($b_i$, $b_{ij}$ ...) are obtained from system response data (Table 4), using the following equation:

$$b_0 = \frac{1}{N} \sum_{u=1}^{N} Y_u \quad (3)$$

$$b_i = \frac{1}{N} \sum_{u=1}^{N} X_{iu} Y_u \quad (4)$$

$$b_{ij} = \frac{1}{N} \sum_{u=1}^{N} X_{iu} \cdot X_{ju} \cdot Y_u \quad (5)$$

Control of reproducibility of experiments and evaluation of experimental error were performed by repeating experiments in the plan center (zero level of factors $X_2$ and $X_3$), using 95% confidence level. Since one factor, $X_1$, was milling ball material ($SiO_2$ or $Al_2O_3$) which would have as zero level mixture of these two different types, repeating of experiments in the plan center was made separately for both types, taking the greater experimental error as a basis for evaluation of statistical significance of regression coefficients ($b_i$) by the Student t-test. Model adequacy was verified according to the Fisher F-test,[11,12] comparing the table values of $F_t$ with calculated values of $F_r$, for respective degrees of freedom.

### 3.2 Empirical statistical models

It can be seen from Table 4 that the ball milling type, as well as sintering temperature has quite a significant influence on sintering and devitrification processes. The devitrification process is more intensive in the case of $Al_2O_3$ balls (higher impurities content) and that also has an influence on the sintering process, i.e. on density, porosity and strength of sintered samples.

On the basis of the results shown in Table 4, statistical models were formed, (Table 5).[8,9] They give the relations between sintered samples properties and ball milling type (i.e. impurities content), temperature and time of sintering. In these models, having the general form given by eqn (2), only coefficients with 95% level of significance, according to the Student t-test were included:

$$Y_1 = 1{\cdot}9376 + 0{\cdot}018125\ X_2 + 0{\cdot}009125\ X_3 \ldots\ldots (6)$$

$$Y_2 = 11{\cdot}4 \ldots\ldots\ldots \quad (7)$$

$$Y_3 = 281{\cdot}1 - 66{\cdot}425\ X_1X_2 - 21{\cdot}675\ X_2X_3 \ldots\ldots (8)$$

$$Y_4 = 13{\cdot}1 - 3{\cdot}725\ X_2 \ldots\ldots \quad (9)$$

$$Y_5 = 28{\cdot}1 + 11{\cdot}925\ X_1 + 20{\cdot}35\ X_2 + 3{\cdot}95\ X_3 + 7{\cdot}0\ X_1X_2 + 2{\cdot}725\ X_2X_3 \ldots\ldots (10)$$

It can be easily seen that, in the investigated interval of influencing factors, the most pronounced effect was in the case of cristobalite content ($Y_5$), while in the case of open porosity ($Y_2$) there is no statistically significant (95%) influence of any factor. The comparison between experimental and

**Table 4.** The properties of sintered samples as a function of different sintering conditions and ball milling material

| *Experiment No.* | *Ball milling material* | *Sintering temperature (°C)* | *Sintering time (h)* | *Density (g cm$^{-3}$)* | *Open porosity (%)* | *Compressive strength (MPa)* | *Tensile strength (MPa)* | *Cristobalite content (vol.%)* |
|---|---|---|---|---|---|---|---|---|
| 1 | $SiO_2$ | 1175 | 1 | 1·905 | 12·4 | 151·0 | 15·6 | 1·5 |
| 2 | $SiO_2$ | 1175 | 3 | 1·935 | 10·7 | 255·1 | 18·8 | 4·2 |
| 3 | $SiO_2$ | 1275 | 1 | 1·948 | 10·5 | 345·4 | 12·1 | 20·8 |
| 4 | $SiO_2$ | 1275 | 3 | 1·974 | 9·5 | 325·2 | 9·5 | 38·3 |
| 5 | $Al_2O_3$ | 1175 | 1 | 1·915 | 11·7 | 363·5 | 20·4 | 11·6 |
| 6 | $Al_2O_3$ | 1175 | 3 | 1·923 | 11·6 | 356·2 | 12·7 | 13·8 |
| 7 | $Al_2O_3$ | 1275 | 1 | 1·946 | 13·0 | 254·2 | 8·4 | 62·8 |
| 8 | $Al_2O_3$ | 1275 | 3 | 1·955 | 11·9 | 198·6 | 7·7 | 72·0 |

**Table 5.** Coding of factors and system responses

| *Factors* | *Responses* |
|---|---|
| $X_1$ — Type of milling balls (Impurity content) | $Y_1$ — Density (g cm$^{-3}$) |
| | $Y_2$ — Open porosity (%) |
| $X_1$ = −1 $SiO_2$ balls | |
| $X_1$ = +1 $Al_2O_3$ balls | $Y_3$— Compressive strength $\sigma_c$ (MPa) |
| $X_2$ — Sintering temperature | |
| $X_2$ = −1 1175°C | $Y_4$ —Tensile strength |
| $X_2$ = +1 1275°C | $\sigma_t$ (MPa) |
| $X_3$ — Sintering time | |
| $X_3$ = −1 1 h | $Y_5$ — Cristobalite content |
| $X_3$ = +1 3 h | (vol.%) |

calculated values of responses from the models is given in Table 6. By testing of model adequacy, according to Fisher F-test, it was established that all obtained models are adequate ($F_r<F_t$), even the model for open porosity (OP=constant) because of small differences in porosity of sintered samples, Table 6. The compressive strength model shows the influence of all three factors, while in the case of tensile strength only the influence of sintering temperature has the statistical significance. In the case of cristobalite content model there is a significant influence of all factors, including interaction of factors. That fact points out the necessity and possibility of very precise control of cristobalite content in sintered samples.

By projecting the response surfaces on the plane temperature–time it is possible to obtain the contour plots. Figure 1 shows contour plots for density, compressive strength, and cristobalite content. The diagram for density is the same for both milling ball types. For the cristobalite content and compressive strength the diagrams are different because the milling ball type, i.e. impurities content, has a significant influence on the devitrification process.

From the contour plots for compressive strength it is evident that for $SiO_2$ balls (lower impurities content) the strength continuously increases, and for $Al_2O_3$ balls (higher impurities content) the strength continuously decreases. This is more illustrative in Fig. 2, where 3D response surfaces for compressive strength and cristobalite content are given. These characteristics cannot be connected with the character of density change, having a continuous increase, and it is even more difficult with a minimum change in the open porosity. In the case of higher cristobalite content the density increase of sintered samples should be attributed to the density change due to the phase transformation because of the difference between density of fused silica (2·20 g·cm$^{-3}$) and cristobalite (2·33 g·cm$^{-3}$). In the same way this should be taken into account for the analysis of porosity change. By calculating the density of crystallized fused silica $\rho_{th}$ (the mixture of fused $SiO_2$ and cristobalite), total and closed porosity, it can be seen that during firing part of the open pore closes (by viscous flow mechanism — typical for the glassy system) but there is almost no change in total porosity, Table 7.

The strength changes of sintered samples evidently could not be the consequence of different porosity. In this case there is a greater influence of strengthening of contacts between particles during sintering, as well as of lower cristobalite content, while the decrease is connected with the exaggerated cristobalite content, when even macro flaws arise.

Analysis of contour plots for compressive strength and cristobalite content for both ball milling types enables us to register the existence of a direct connection between strength change and cristobalite content.

Diagrams of compressive and tensile strength as a function of cristobalite content in sintered samples, for both ball milling types together, are shown in Figs 3 and 4.

Tensile strength is more sensitive to the cristobalite content change in the region of maximum,

**Table 6.** Adequacy test of statistical models

| *Experiment No.* | *Density (g cm$^{-3}$)* $Y_1$ | | *Open porosity (%)* $Y_2$ | | *Compressive strength (MPa)* $Y_3$ | | *Tensile strength (MPa)* $Y_4$ | | *Cristobalite content (vol.%)* $Y_5$ | |
|---|---|---|---|---|---|---|---|---|---|---|
| | *Exp.* | *Cal.* | *Exp.* | *Cal.* | *Exp.* | *Cal.* | *Exp.* | *Cal.* | *Exp.* | *Cal.* |
| 1 | 1·905 | 1·910 | 12·4 | 11·4 | 151·0 | 193·0 | 15·6 | 16·8 | 1·5 | 1·6 |
| 2 | 1·935 | 1·929 | 10·7 | 11·4 | 255·1 | 236·3 | 18·8 | 16·8 | 4·2 | 4·0 |
| 3 | 1·948 | 1·947 | 10·5 | 11·4 | 345·4 | 369·2 | 12·1 | 9·4 | 20·8 | 22·8 |
| 4 | 1·974 | 1·965 | 9·5 | 11·4 | 325·2 | 325·8 | 9·5 | 9·4 | 38·3 | 36·2 |
| 5 | 1·915 | 1·910 | 11·7 | 11·4 | 363·5 | 325·8 | 20·4 | 16·8 | 11·6 | 11·4 |
| 6 | 1·923 | 1·929 | 11·6 | 11·4 | 356·2 | 369·2 | 12·7 | 16·8 | 13·8 | 13·9 |
| 7 | 1·946 | 1·947 | 13·0 | 11·4 | 254·2 | 236·3 | 8·4 | 9·4 | 62·8 | 60·7 |
| 8 | 1·955 | 1·965 | 11·9 | 11·4 | 198·6 | 193·0 | 7·7 | 9·4 | 72·0 | 74·0 |
| $F_r$ | 1·6 | | 6·25 | | 3·07 | | 1·6 | | 3·8 | |
| $F_t$ | 9·2 | | 9·2 | | 9·2 | | 9·2 | | 9·2 | |
| | Adequate | | Adequate | | Adequate | | Adequate | | Adequate | |

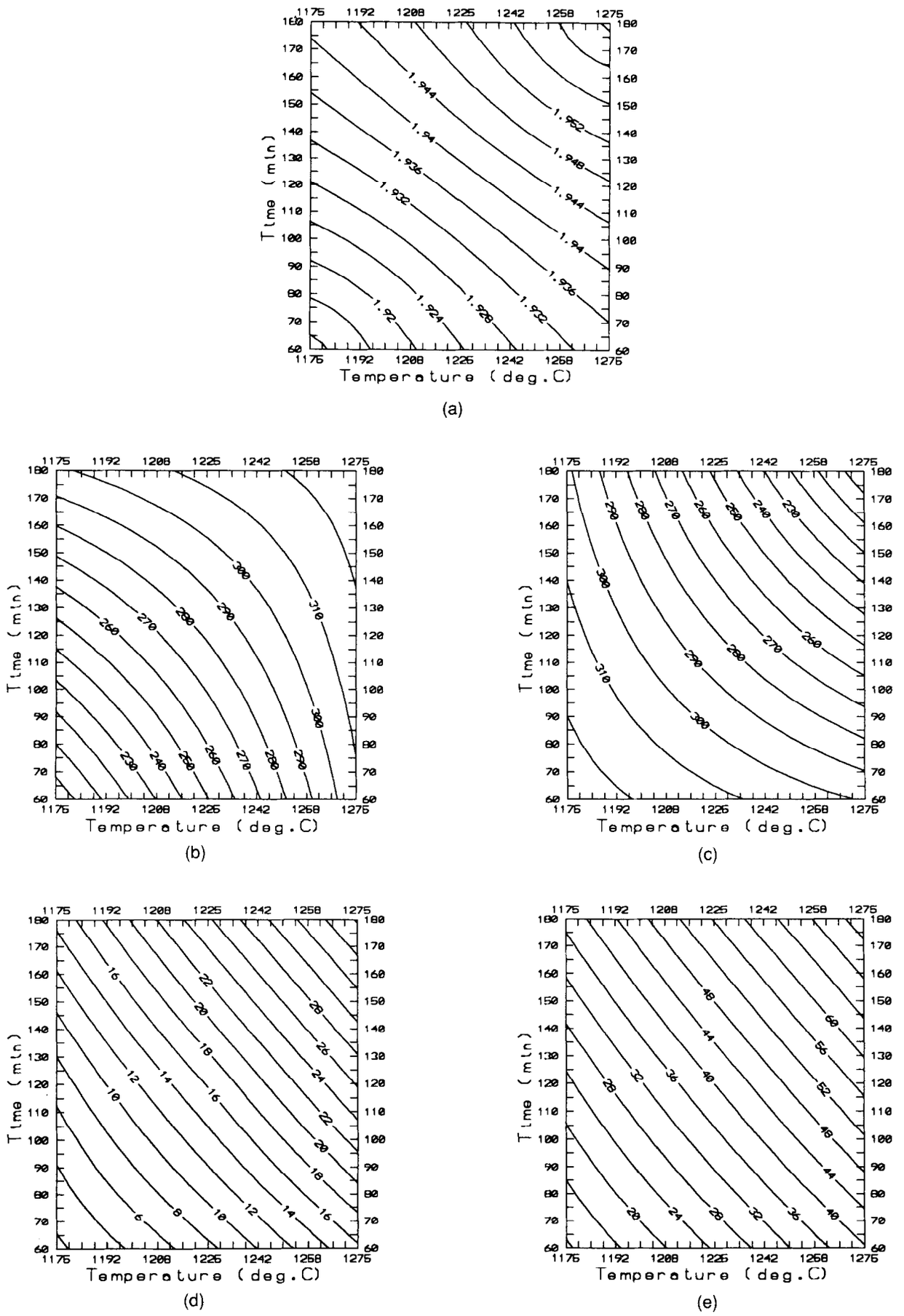


**Fig. 1.** Contour plots of response surfaces for mathematical models — relations between sintered samples properties and sintering conditions and impurities content. (a) Density (g cm $^{3}$); (b) Compressive strength (MPa) — $SiO_2$ balls; (c) Compressive strength (MPa) — $Al_2O_3$ balls; (d) Cristobalite content (vol.%) — $SiO_2$ balls; (e) Cristobalite content (vol.%) — $Al_2O_3$ balls.

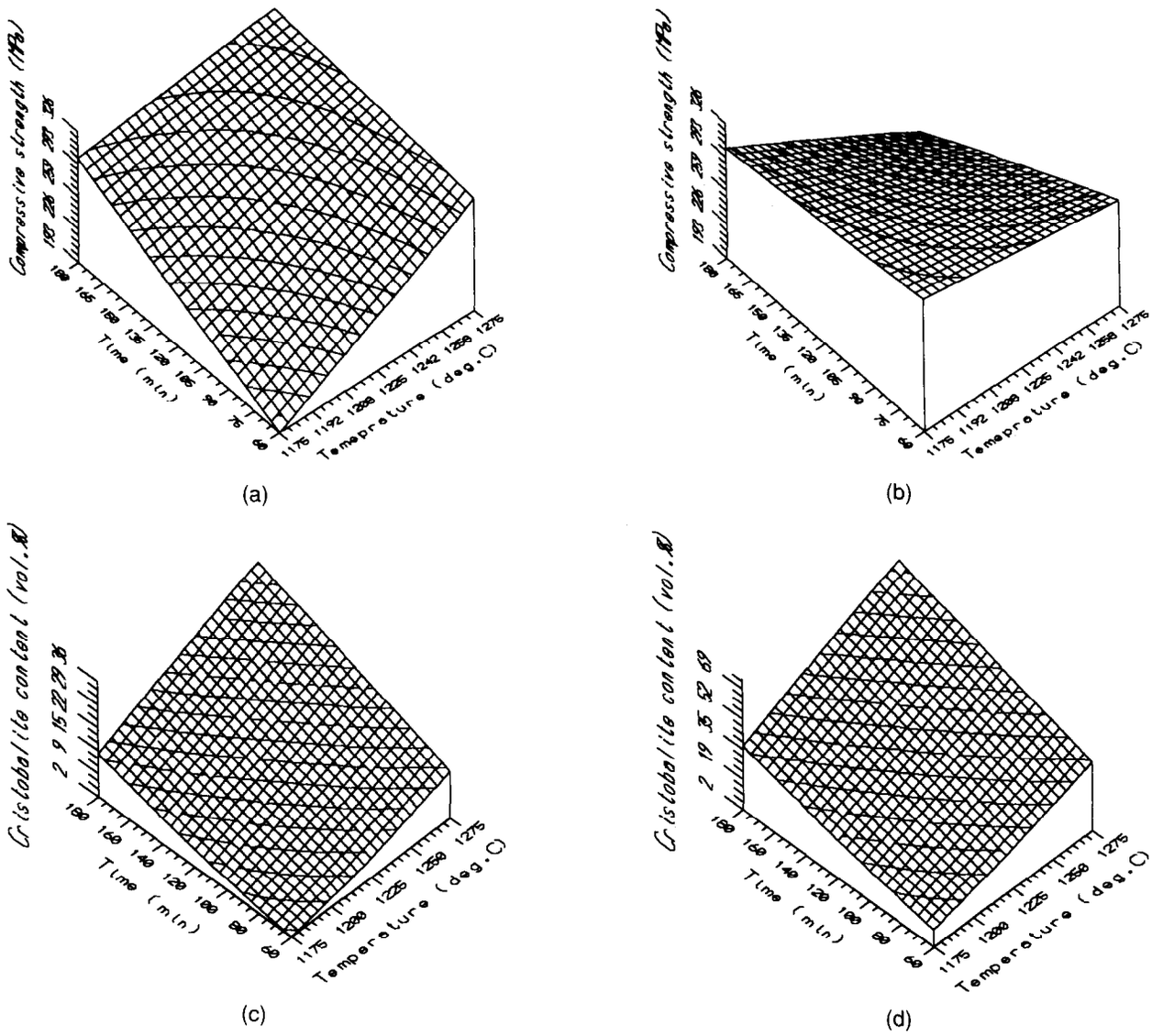


**Fig. 2.** Response surfaces for compressive strength and cristobalite content as a function of temperature and time of sintering for different ball milling material. (a) Compressive strength (MPa) — $SiO_2$ balls; (b) Compressive strength (MPa) — $Al_2O_3$ balls; (c) Cristobalite content (vol.% ) — $SiO_2$ balls; (d) Cristobalite content (vol.%) — $Al_2O_3$ balls.

**Table 7.** Analysis of sintered samples porosity

| *Experiment No.* | *Cristobalite content (vol.%)* | $\rho_{th}$ *(g cm* $^{3}$*)* | $\rho_{exp}$ *(g cm* $^{3}$*)* | *Porosity (%)* | | |
|---|---|---|---|---|---|---|
| | | | | *Total* | *Open* | *Closed* |
| 1 | 1·5 | 2·202 | 1·905 | 13·5 | 12·4 | 1·1 |
| 2 | 4·2 | 2·205 | 1·935 | 12·2 | 10·7 | 1·5 |
| 3 | 20·8 | 2·227 | 1·948 | 12·5 | 10·5 | 2·8 |
| 4 | 38·3 | 2·250 | 1·974 | 12·3 | 9·5 | 2·8 |
| 5 | 11·6 | 2·215 | 1·915 | 13·5 | 11·7 | 1·8 |
| 6 | 13·8 | 2·218 | 1·923 | 13·3 | 11·6 | 1·7 |
| 7 | 62·8 | 2·282 | 1·946 | 14·7 | 13·0 | 1·7 |
| 8 | 72·0 | 2·294 | 1·955 | 14·8 | 11·9 | 2·9 |

so it is possible from Fig. 4 to establish the most convenient cristobalite content very precisely and then, using a contour plot for cristobalite content, to find out the region of optimum combination for sintering conditions. It could be concluded that the optimum content of cristobalite is 6–8 vol.% and in Fig. 1(d) (for $SiO_2$ balls) the corresponding region of proper combination of sintering

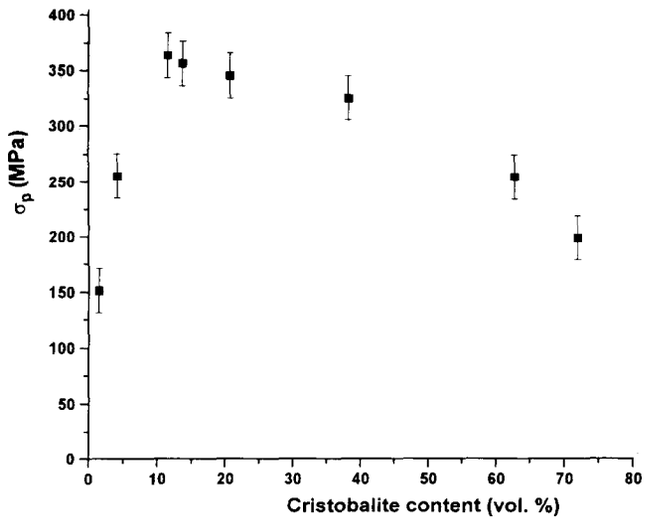


**Fig. 3.** Compressive strength of sintered samples as a function of cristobalite content.

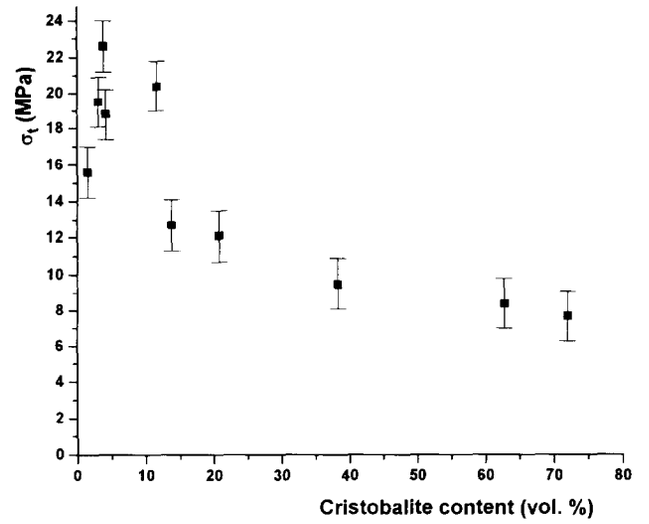


**Fig. 4.** Tensile strength of sintered samples as a function of cristobalite content.

conditions (temperature and time) should be found near the corner 1175°C, 1 h. It should be pointed out that it is necessary to control the temperature very precisely. For $Al_2O_3$ balls the optimum region is outside of investigated factorial space (temperatures lower than 1175°C) so further experiments are required to find such a combination for sintering temperature and time.

## 4 Conclusions

The study of sintering and devitrification processes of fused silica has shown that the interaction of these two processes is strongly dependent on impurities content. Up to a certain level these two processes support each other, and after this the sintering process is retarded by devitrification. Forming of cristobalite causes a density increase of sintered samples while porosity remains practicaly unchanged.

The strength increase is connected with the strengthening of the contacts between grains due to the sintering, by the viscous flow mechanism, and forming of small quantities of cristobalite. The relations between sintered samples properties and sintering conditions and impurities content were established using statistical modelling by the multifactorial experimental design. Using analysis of response surfaces of these models and correlation of the compressive strength and tensile strength with cristobalite content it was established that for 6–8 vol.% cristobalite the strength of sintered samples has the maximum values. Tensile strength is more sensitive to the cristobalite content so this property should be the criterion for establishing the optimum sintering conditions.

## Acknowledgements

The authors wish to acknowledge S. Zec for cristobalite content determination in samples. This work was supported by the Scientific Fund of the Republic of Serbia, within the project No. 905.

## References

1. Pivinskij, Yu. E. & Romašin, A. G., *Kvarcevaja Keramika*, Metallurgija, Moskva, 1974.
2. Walton, J. D., Sintered Fused Silica, *Interceram*, **2** (1968) 121–122, 133.
3. Kappmeyer, K. K., Russel, C. K. & Hubble, D. H., Refractories for Continuous Casting. *Amer. Ceram. Soc. Bull.*, **53** (1974) 519–523, 527.
4. Ah'jan, A. M., O nekotoryh oblastjah primenenija kvarcevoj keramiki. *Ogneupory* (1982) 4, 40–44.
5. Harris, J. N. & Welsh, E. A., *Fused Silica Design Manual*, Vol. I., Eng. Exp. Station, Georgia Inst. of Technology, Atlanta, 1973.
6. Wagstaff, F. E., Kinetics of Crystallization of Vitreous Silica, PhD Thesis, University of Utah, 1962.
7. Gašić, M., Kićević, D. & Klecko, G., The Structural Changes of Amorphous $SiO_2$ Powders. In *Contemporary Inorganic Materials*, ed. G. Petzow & W. J. Huppmann. Riederer Verlag GmbH, Stuttgart, 1978, pp. 11–17.
8. Katanić-Popović, J. & Stevanović, M., Measuring the Strength of Brittle Materials by Diametral Compression Method. *Refractories* (in Serb.), **1** (1971) 31–4.
9. Harris, J. N. & Welsh, E. A., *Acceptance Criteria for Slip-cast Fused Silica Radomes*. Tech. Rep. No. 3, Contract N 00017-70-C-4438, Georgia Inst. of Technology, Atlanta, June 1972.
10. Kićević, D., Gašić, M., Zec, S. & Marković, D., X-ray Diffraction Method for Quantitative Determination of Cristobalite in Fused Silica. *J. Serb. Chem. Soc.*, **59** (1994) 185–94.
11. Bondar, A. G. & Statjuha, G. A., *Planirovanie eksperimenta v himičeskoj tehnologiji*, Izd. Viša škola, Kiev, 1976., pp. 6–12, 54–82.

12. Box, G. E. P., Hunter, W. G. & Hunter, J. S., *Statistics for Experimenters — An Introduction to Design, Data Analysis and Model Building*, John Wiley and Sons, New York 1978, pp. 306–22, 510–26.

13. Tecilazić-Stevanović, M., Janaćković, T., Kostić-Gvozdenović, Lj. & Ćirjaković, R., Dependence of the Properties of Cordierite–Mullite Ceramics on Synthesis Conditions. *Ind. Ceramics*, **13** (1993) 31–4.